Progress In Electromagnetics Research C, Vol. 131, 241–257, 2023

A Novel Receiving Subarray Partition Layout Model for Microwave Power Transmission with Smaller Power Dispersion

Jianxiong Li[1, 2, *] and Wen Qin[1, 2]

Abstract—A novel subarray layout method is proposed for the problems of high power dispersion and high complexity of the existing layout methods of receiving rectifier antenna arrays. By the traditional RF synthesis and DC synthesis array layout, the number of units used is high, and the received power dispersion is high. Therefore, this paper proposes a uniform non-overlapping triangular subarray partition layout, and the layout takes three discrete parameters of subarray type, subarray position, subarray placement direction as optimization variables. The minimum dispersion of the received power of the subarray is used as the optimization objective to establish the optimization model. We adopt the Taboo Search (TS) algorithm to achieve the global optimum by setting up a taboo table for global neighborhood search and homogenize the received microwave power value from each subarray. The result shows a lower coefficient of variation (CV) with fewer subarrays and a globally symmetric subarray layout, which reduces the engineering complexity and cost of the subsequent rectification circuit, as well as a lower dimensional span between different subarray types in this novel subarray layout model. We conducted a series of numerical simulations to prove that the method can meet the requirement of minimum power dispersion while ensuring that the total reception efficiency will not be greatly reduced, which verifies the effectiveness of this receiving subarray layout method.

1. INTRODUCTION

A typical Microwave Wireless Power Transmission (MWPT) system consists of two major components: (1) Microwave transmitting antenna system. It consists of a microwave source (DC-MW) and a transmitting antenna, which can convert DC electrical energy into microwave energy and transmit it into the free space. (2) Receiving and rectifying antenna system. It consists of a receiving antenna, a rectifier circuit, and a DC synthesizer circuit, which can receive microwave energy in free space and convert it to DC [1–3]. The receiving conversion efficiency of a receiving rectifier antenna, as an important part of the microwave energy transmission link, directly affects the efficiency of the entire energy transfer system. An excellent receiving rectifier antenna often requires high rectification efficiency, stable working condition, and compact structure form [4, 5].

This paper focuses on a receiving antenna array in a rectifier antenna system, for the present, receiving rectifier antenna mostly in the form of array. Its receiving rectification efficiency is mainly composed of two parts: antenna receiving efficiency and rectification circuit rectification efficiency. The high conversion efficiency of the rectifier circuit is the focus of the receiving rectifier antenna research. This is because the nonlinearity of the rectifier circuit decides that it is very sensitive to both input power and load [6–8]. However, on the one hand, the irradiated power density from the transmitting antenna to the receiving antenna area is usually uneven, and if the uneven power is fed into the rectifier

Received 18 January 2023, Accepted 18 March 2023, Scheduled 1 April 2023

* Corresponding author: Jianxiong Li (lijianxiong@tiangong.edu.cn).

[1] School of Electronics and Information Engineering, Tiangong University, Tianjin, China. [2] Tianjin Key Laboratory of Optoelectronic Detection Technology and Systems, Tianjin, China.

circuit, the power mismatch will make the rectifier circuit conversion efficiency low in many areas [9–11]. On the other hand, if the load cannot be matched with the rectifier circuit, it will also cause low rectification efficiency. Therefore, the homogenization of the received power in different areas of the receiving antenna array and the degree of matching between the rectifier circuit and the load both limit the efficiency of the receiving rectifier antenna system. Therefore, the array layout method research for the homogenization of the received power of the receiving antenna array is of great importance for the construction of an efficient microwave energy transmission system [12–14]. So far, the array layout has two main configurations: (1) The RF power received by all antenna elements through the microwave power distribution network is combined and then transmitted to the rectifier. For large antenna arrays, although this configuration requires only one rectifier, the power distribution network is very complex and has huge power losses. (2) The RF power from each antenna element is rectified to DC power through each rectifier separately, and then the DC energy is combined together by the DC series-parallel method [15–17]. This configuration avoids the use of complex power distribution networks. However, the power density of the transmitting antenna irradiated at the receiving antenna aperture is usually not uniform [18]. When the same rectifier is used, the rectifier efficiency is reduced due to power mismatch between the receiving antenna and the rectifier [19, 20].

Therefore, we need a corresponding subarray partition of the receiving antenna array to ensure the better homogenization of the received power. It also ensures that the overall reception efficiency is not reduced too much. A uniform non-overlapping rectangular subarray partition based on the path traversal algorithm is proposed in [10]. The coefficient of variation (CV) denotes the ratio of the standard deviation of the received power of the subarray to the average of the received power of the subarray. The smaller the CV represents the less discrete data and the better homogenization effect. In this paper, we propose a uniform non-overlapping triangular subarray partition based on the Taboo Search (TS) algorithm. Uniform non-overlap means that the number of array elements of each type of subarray remains the same and that the subarray graph elements are independent of each other and have no intersection. The use of triangular subarrays can appropriately reduce the number of iterations in the subsequent optimization process, thus reducing the computational effort and the complexity of the system. Based on Friis equation [12], we firstly establish the subarray received power calculation model, and secondly establish the layout model with subarray received power homogenization as the optimization objective and use the TS algorithm to solve it. We arrange the first quadrant and simulate the initialized layout with 22 rectangular subarrays. Next, we perform global neighborhood search and stepwise optimization according to the optimization objective, iterate in the rectangular subarrays in a loop, and perform the cutting of triangular subarrays to derive the optimal subarray layout model under different reference values, and finally, we perform global symmetry and use less number of subarrays, which greatly reduces the subsequent rectifier circuit. This greatly reduces the engineering complexity of the subsequent rectifier circuit. At the same time, the actual received power distribution of each subarray antenna under each reference value is simulated, and eventually the minimum CV simulation value reaches 0.1581, which verifies the effectiveness of the layout model proposed in this paper.

The contributions of this paper are mainly in the following aspects. Firstly, a novel triangular partition model is proposed based on the ideology of graph elements. And an optimization method different from that in [10] is used. We give a procedure diagram of the algorithm, and the model is solved by the TS algorithm. It makes the subarray received power less dispersion, and it can also ensure high reception efficiency. Secondly, in order to further explore the effect of reference value (ε_{rec}) on the synthesis results and highlight the advantages of the novel subarray layout, we simulated the rectangular subarray layout and triangular subarray layout under different ε_{rec}. Finally, we synthesize and compare several existing receiving array layouts. In conclusion, the uniform non-overlapping triangular subarray partition based on TS algorithm is more suitable as the receiving array of the MWPT system.

2. MATHEMATICAL MODEL OF THE RECEIVED POWER OF THE ANTENNA ARRAY

2.1. MWPT Transceiver Array System Model Based on Receiving Subarray

Fig. 1 shows a transceiver antenna model of the MWPT system. The system consists of a transmitting array antenna and a receiving array antenna. The latter is composed of a number of subarrays. The

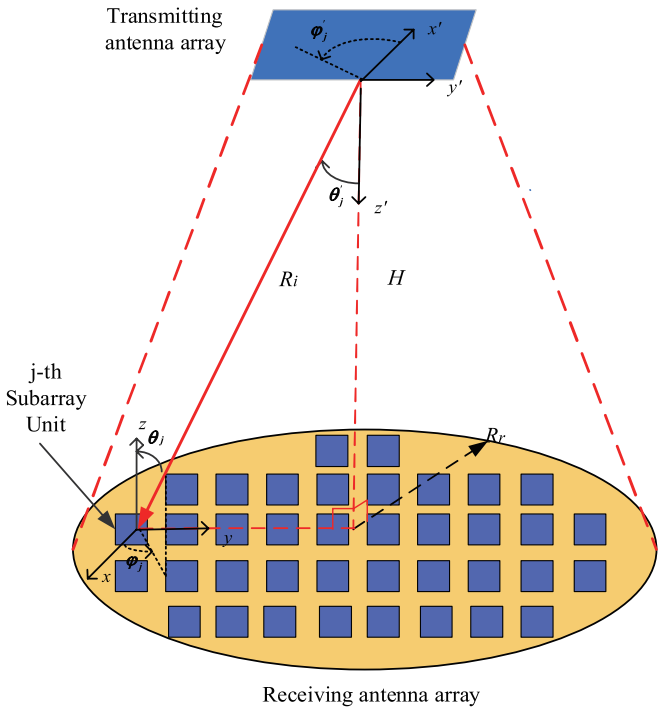

Figure 1. The model of MWPT system.

distance between the transmitting end and receiving end is H. The radius of the receiving area is R_r. Two planes of transmitting array antenna and receiving array antenna are parallel to each other. Their geometric centers are coaxial.

The geometric relationship between the relative positions of the j-th receiving subarray and the transmitting antenna array is also shown in Fig. 1. In the figure, θ_j and φ_j indicate the pitch and direction angles of the j-th subarray in the coordinate system relative to the position of the transmitting array, respectively. θ'_j and φ'_j denote the pitch and direction angles of the transmitting array antenna in the coordinate system relative to the j-th subarray position, respectively. Fig. 2 shows the different subarray types used in Fig. 1 for the layout of the receiving array.

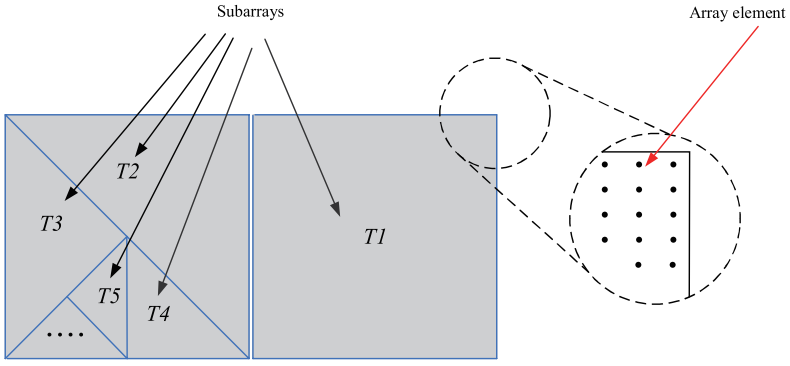

Figure 2. Subarray of different types.

In Fig. 2, $T_i \in T = \{T_1, T_2, \cdots, T_k\}$ denotes the i-th subarray type. Through Fig. 2 we can see that there is a dimensional connection between different types of subarray, and the subarray with larger dimension can get two subarrays with smaller dimension by dichotomy.

2.2. Subarray Received Power Calculation Model

For the subarray depicted in Fig. 1, the received power calculation can be expressed as [12]:

$$P_j^{sub} = S_j^{sub} \cdot A_j^e \cdot \rho_j \tag{1}$$

where S_j^{sub} represents the power density irradiated to the j-th subarray, A_j^e the effective aperture area of this subarray, ρ_j the polarization mismatch factor of this subarray and the transmitting array antenna [10]. They can be expressed as:

$$S_j^{sub}\left(\theta_j', \varphi_j'\right) = \frac{G_t\left(\theta_j', \varphi_j'\right) P_t}{4\pi R^2} \tag{2}$$

$$A_j^e\left(\theta_j, \varphi_j\right) = \frac{G_j^{sub}\left(\theta_j, \varphi_j\right) \lambda^2}{4\pi} \tag{3}$$

$$\rho_j = \left|\cos\psi_p\right|^2 = \frac{\left|\mathbf{E}_t \cdot \mathbf{h}_j\right|^2}{\left|\mathbf{E}_t\right|^2 \cdot \left|\mathbf{h}_j\right|^2} \tag{4}$$

where P_t is the radiated power of the transmitting antenna array; $G_t\left(\theta_j', \varphi_j'\right)$ and $G_j^{sub}\left(\theta_j, \varphi_j\right)$ denote the gain of the transmitter in the direction of $\left(\theta_j', \varphi_j'\right)$ and the gain of the j-th subarray of the receiver in the direction of (θ_j, φ_j), respectively. $\mathbf{E}_t$ is the electric field vector of the transmitting array, $\mathbf{h}_j$ the polarization vector of the receiving subarray, and ψ_p the angle between $\mathbf{E}_t$ and $\mathbf{h}_j$. For transverse electromagnetic waves, the incoming electric field $\mathbf{E}_t$ and polarization vector $\mathbf{h}_j$ of the receiving antenna at a particular moment and space position can be expressed in the spherical coordinate system as [22]:

$$\mathbf{h}_j = h_0\left(a_0 + \rho_1 e^{j\beta_1} a_\phi\right) \tag{5}$$

$$\mathbf{E}_t = E_0\left(a_0 + \rho_2 e^{j\beta_2} a_\phi\right) \tag{6}$$

If the standard parameter polarization ratio and the initial phase difference are used to represent the polarization mismatch factor method, the above equation can be expressed as [22]:

$$\rho_j = \frac{\left[1+\rho_1\rho_2\cos(\beta_1+\beta_2)\right]^2 + \left[\rho_1\rho_2\sin(\beta_1+\beta_2)\right]^2}{\left(1+\rho_1^2\right)\cdot\left(1+\rho_2^2\right)} = \frac{\left[1+\rho_t\rho_j^{sub}\cos\left(\beta_t+\beta_j^{sub}\right)\right]^2 + \left[1+\rho_t\rho_j^{sub}\sin\left(\beta_t+\beta_j^{sub}\right)\right]^2}{\left(1+\rho_t^2\right)\cdot\left(1+\left(\rho_j^{sub}\right)^2\right)} \tag{7}$$

where ρ_t and ρ_j^{sub} are polarization ratios of the transmitting array and j-th subarray; β_t and β_j^{sub} are the initial phase differences of the two orthogonal components of the respective electric field vectors of the transmitting array and the j-th subarray. Combining the above mathematical expressions, the formula for calculating the received power of the j-th subarray can be expressed as:

$$P_j^{sub} = \frac{P_t G_j^{sub}\left(\theta_j, \varphi_j\right) G_t\left(\theta_j', \varphi_j'\right) \lambda^2}{\left(4\pi R\right)^2} \cdot \frac{\left[1+\rho_t\rho_j^{sub}\cos\left(\beta_t+\beta_j^{sub}\right)\right]^2 + \left[1+\rho_t\rho_j^{sub}\sin\left(\beta_t+\beta_j^{sub}\right)\right]^2}{\left(1+\rho_t^2\right)\cdot\left(1+\left(\rho_j^{sub}\right)^2\right)} \tag{8}$$

where the gain G of the transmitter and receiver can be expressed as [21]:

$$G\left(\theta, \varphi\right) = 3.136\left\{\sin\theta \frac{\sin\left(\frac{\pi}{2}\cos\theta\right)}{\cos\theta}\cos\left(\frac{\pi}{2}\sin\theta\sin\varphi\right)\right\}^2 \tag{9}$$

The total received power of the receiving array can be obtained by synthesizing the received power of all subarray as:

$$P_r = \sum_{j=1}^{J} P_j^{sub} \tag{10}$$

In addition, the total power irradiated to the receiving array can be obtained by double integration of the irradiated power density within the receiving array aperture, and it can be written as:

$$P_r^{rad} = \iint\limits_{B_1} S_j^{sub}\left(\theta_j', \varphi_j'\right) ds + \iint\limits_{B_2} S_j^{sub}\left(\theta_j', \varphi_j'\right) ds + \cdots \iint\limits_{B_j} S_j^{sub}\left(\theta_j', \varphi_j'\right) ds = \sum_{j=1}^{J} \iint\limits_{B_j} S_j^{sub}\left(\theta_j', \varphi_j'\right) ds \quad (11)$$

where B_j denotes the finite closed region of the j-th subarray. According to [10], the power density approximate distribution of the received array aperture field irradiation can be obtained in Fig. 3.

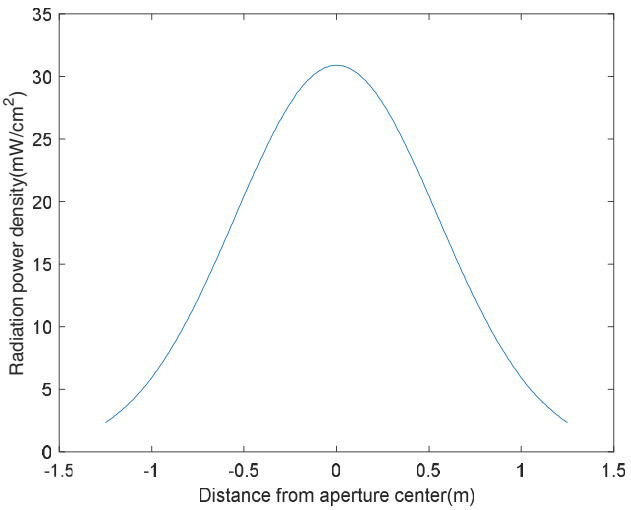

Figure 3. 2D power density distribution.

3. THE ESTABLISHMENT AND SOLUTION OF SUBARRAY LAYOUT OPTIMIZATION MODEL

3.1. Mathematical Model

Due to the inhomogeneity of the irradiated power density within the receiving array aperture field, we need to use subarrays of different types to receive energy from different areas. Eventually we can achieve the homogenization of the received power of the subarrays. Therefore, the following elaboration is required for the subarray layout model.

(1) We need to consider the subarray position, subarray type, and subarray placement direction as one of the optimization variables.
(2) The homogenization of subarray received power also means minimizing subarray received power dispersion as the optimization aim. However, by considering the power loss of the subarray, we need to take the reception efficiency into consideration, so the reception efficiency maximization is also used as the optimization aim in the layout model. The subarray layout optimization problem is a multi-objective optimization problem.
(3) The subarray layout problem can be categorized as a two-dimensional layout optimization problem with geometric constraints, and it also implies that the graph elements do not interfere with each other, as shown in Fig. 4.

In Fig. 4, the circular area can be denoted as: $\mathbf{B} = \left\{(x, y) \,|0 < x^2 + y^2 \leq r^2\right\}$. Several graph elements in the region are denoted by v_j, $j \in I_J = \{1, 2, \cdots, J\}$, where J is the total number of graph elements. $\hat{p}_j = (x_j, y_j) \in \mathbf{B}$, which is the coordinate of the shape-center position of v_j; $\hat{t}_j \in \mathbf{T}$ can be used to describe the dimension of the graph. For example, the graph is an arbitrary triangle, so $\hat{t}_j = \{(\omega_j, l_j, k_j) \,|0 < \omega_j \leq l_j \leq k_j\} \in \mathbf{T}$, where ω_j, l_j, k_j denote the lengths of the three sides of the

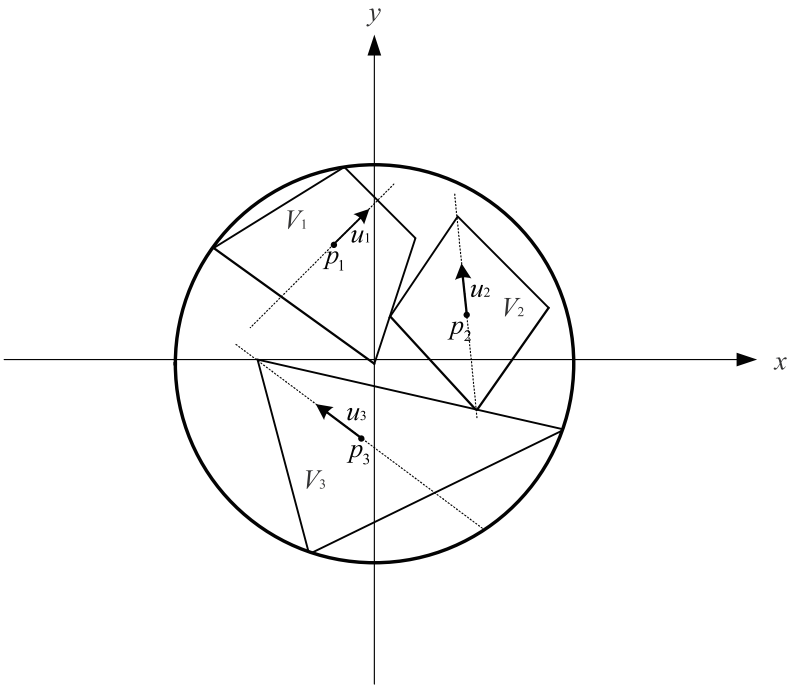

Figure 4. Two-dimensional layout model diagram.

triangle respectively, and the lengths are in increasing order. $\hat{u}_j$ is used to describe the placement direction of the subarray, $\|\hat{u}_j\| = 1$, and $\hat{u}_j$ is parallel to the longest cut line passing through the V_j-shaped center $\hat{p}_j$. Therefore, each graph element v_j can be uniquely determined by its corresponding $\hat{p}_j$, $\hat{t}_j$, $\hat{u}_j$. Based on the above facts, we can derive the subarray layout optimization model:

$$
\begin{aligned}
&\textit{find} \quad V = \{\mathbf{P}, \mathbf{T}, \mathbf{U}\}^H = \left\{\hat{p_1}, \hat{p_2}, \cdots, \hat{p_j}, \hat{t_1}, \hat{t_2}, \ldots, \hat{t_j}, \hat{u_1}, \hat{u_2}, \cdots, \hat{u_j}\right\}^H \\
&\textit{minimize} \quad \left|P_r - P_r^{rad}\right| \\
&\textit{minimize} \quad CV = \sqrt{\frac{\sum_{j=1}^{J}\left(P_j^{sub} - \left(\sum_{j=1}^{J} P_j^{sub}\right)\Big/ J\right)^2}{M}}\Bigg/\left(\sum_{j=1}^{J} P_j^{sub}\right)\Bigg/ J \\
&\textit{subject} \quad \text{(a) } \operatorname{int}(v_{j1}) \cap \operatorname{int}(v_{j2}) = \emptyset \quad j1 \neq j2 \\
&\qquad\qquad \text{(b) } j1, j2 \in \{1, 2, \cdots, J\} \\
&\qquad\qquad \text{(c) } \hat{p_j} \in \mathbf{P}, \hat{t_j} \in \mathbf{T}, \hat{u_j} \in \mathbf{U}
\end{aligned}
\tag{12}
$$

where V denotes a layout scheme and is also the optimization variable in this layout model; the number of subarray in this scheme is J; H denotes the sample used to store the shape of the subarray; $v_j = \left\{\hat{p}_j, \hat{t}_j, \hat{u}_j\right\}$ represents the graph element of the j-th subarray; $\hat{p}_j = (x_j, y_j)$ is shape-centered coordinates; $\hat{t}_j = \{(\omega_j, l_j, k_j) \,|0 < \omega_j \leq l_j \leq k_j\}$ is external dimensions; the direction of placement is represented by $\hat{u}_j$. Since it is a uniform non-overlapping subarray partition, we use $\operatorname{int}(v_{j1}) \cap \operatorname{int}(v_{j2}) = \emptyset$ as a constraint, which means that the intersection between subarray graph elements is an empty set.

However, it can be seen from the above that the subarray layout optimization problem is a multi-objective two-dimensional layout optimization problem. Two optimization objectives will make the solution difficult, so we make certain simplifications, assuming that the standard deviation of the received power of the subarray is less than a certain reference value, namely $\varepsilon_r \leq \varepsilon_{rec}$. The optimization objective of minimizing the dispersion of the received power of the subarray can be transformed into a constraint,

which leads to a simplified layout optimization model:

$$\begin{aligned} &\textit{find} \quad V = \{\mathbf{P}, \mathbf{T}, \mathbf{U}\}^H = \left\{\hat{p_1}, \hat{p_2}, \cdots, \hat{p_j}, \hat{t_1}, \hat{t_2}, \ldots, \hat{t_j}, \hat{u_1}, \hat{u_2}, \cdots, \hat{u_j}\right\}^H \\ &\textit{minimize} \quad \left|P_r - P_r^{rad}\right| \\ &\textit{subject} \quad \text{(a) int}\,(v_{j1}) \cap \text{int}\,(v_{j2}) = \emptyset \quad j1 \neq j2 \\ &\qquad \text{(b)}\ \varepsilon_r = \sqrt{\frac{\sum_{j=1}^{J}\left(P_j^{sub} - \left(\sum_{j=1}^{J} P_j^{sub}\right)\Big/ J\right)^2}{M}} \leq \varepsilon_{rec} \\ &\qquad \text{(c)}\ j1, j2 \in \{1, 2, \cdots, J\} \\ &\qquad \text{(d)}\ \hat{p_j} \in \mathbf{P}, \hat{t_j} \in \mathbf{T}, \hat{u_j} \in \mathbf{U} \end{aligned} \tag{13}$$

where CV is measured as an index of the homogenization of the received power of the subarray and is described in the last paragraph of the introduction.

3.2. Optimization Model Solution

In the two-dimensional layout optimization problem, such subarray graph elements are relatively special. If we can establish the mapping relationship between elements and layout space, we can realize the conversion between different graph elements by dividing the large space into small spaces, where B_n represents the n-th local layout space, and T_n represents the n-th subarray graph element, as shown in Fig. 5.

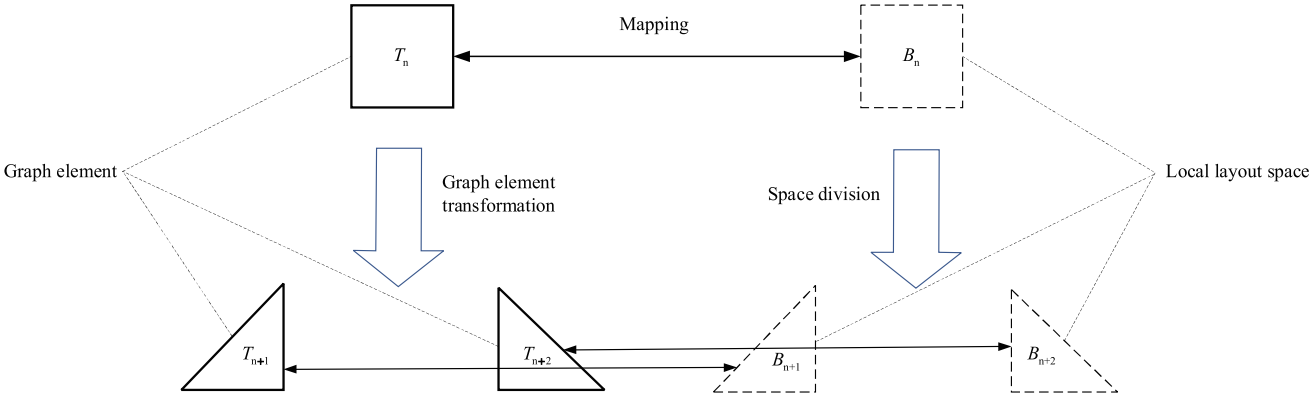

Figure 5. Graph element transformation.

In the subsequent partitioning process, these local spaces will also be divided into smaller spaces, thus generating smaller graph elements. Fig. 6 shows a specific uniform non-overlapping triangular partition model.

Next, we perform global optimization by means of the TS algorithm, and first we identify several important parts of the algorithm:

(1) Neighborhood Function
Neighborhood, as the name implies, is the nearest area to it, and the neighborhood function enables the transformation between different layout schemes. It is assumed that there exists a subarray layout scheme $V = \{v_1, v_2, \cdots, v_n\}$, where the subarray graph element v_1 can be obtained by dichotomizing v_1^1 and v_1^2. Therefore, there must be a neighborhood element named $V^{neig} = \left\{v_1^1, v_1^2, v_2 \cdots, v_n\right\}$ in the neighborhood of $V = \{v_1, v_2, \cdots, v_n\}$, and so on. Each time a subarray is divided, a neighbor element is created, and these elements constitute what we call the neighborhood.

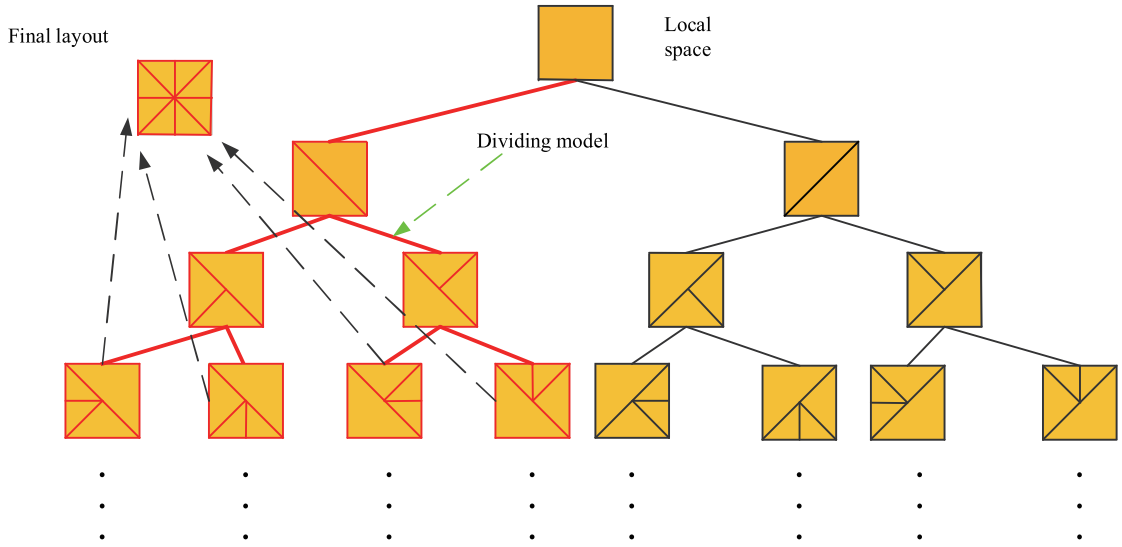

Figure 6. Dividing diagram.

(2) The Initial Layout Scheme
For the subarray layout scheme, the partition between subarray elements through the neighborhood function is often one-way, which means that it must be divided from large subarray elements to small subarray elements, thus we need to first obtain the initial layout scheme by laying down the largest subarray elements in the layout space:

$$V^{ini} = \left\{ \left(\hat{p}_1, \hat{T}_1, \hat{u}_1 \right), \left(\hat{p}_2, \hat{T}_2, \hat{u}_2 \right), \cdots \left(\hat{p}_n, \hat{T}_n, \hat{u}_n \right) \right\} \tag{14}$$

There are n graph elements in this layout scheme, where T_1 indicates that these graph elements are all maximum subarray graph elements.

(3) The Generation Rules of New Layout Scheme
Select a layout solution from the neighborhood of the current layout solution instead of the current layout solution. In this process, guidelines need to be developed so as to ensure global optimization. Therefore, for subarray layout optimization, we can perform the following method:
Firstly, the first v_1-element in V^{ini} which is in the initialized layout is divided to obtain a neighborhood layout scheme called V^{neig} and determine whether it satisfies the restriction in (12) b. Then choose a scheme with the minimum $\left| P_r - P_r^{rad} \right|$ from the old solution V^{ini} and the new solution V^{neig} as the current scheme, which means choosing the layout scheme with the maximum reception efficiency. After that, the next graph element is divided on the basis of this scheme, and the loop is processed sequentially according to the above method. The procedure diagram of the algorithm for subarray layout optimization is shown in Fig. 7.

4. SIMULATION AND RESULTS ANALYSIS

This section is divided into three parts. In the first part, we simulate the novel subarray optimization layout under different reference values. It is the uniform non-overlapping triangular subarray partition layout based on the TS algorithm, and the actual received power distribution of each subarray antenna is simulated under each layout case. Subsequently, we analyze simulation results further through tables and graphs in order to clarify the effect of ε_{rec} on the subarray layout results. The second part is to simulate the layout diagram of uniform non-overlapping rectangular subarray partition based on the path traversal algorithm under the premise of the subarray layout optimization model used in this paper. We will compare the two array models for analysis. The third part is a comprehensive comparison of several existing receiving rectifier antenna arrays. The CPU used for all simulations is Intel(R)Core(TM)i5-1035G1, 1.00 GHz, 8 GB RAM, and the simulation software is MATLAB 2021a.

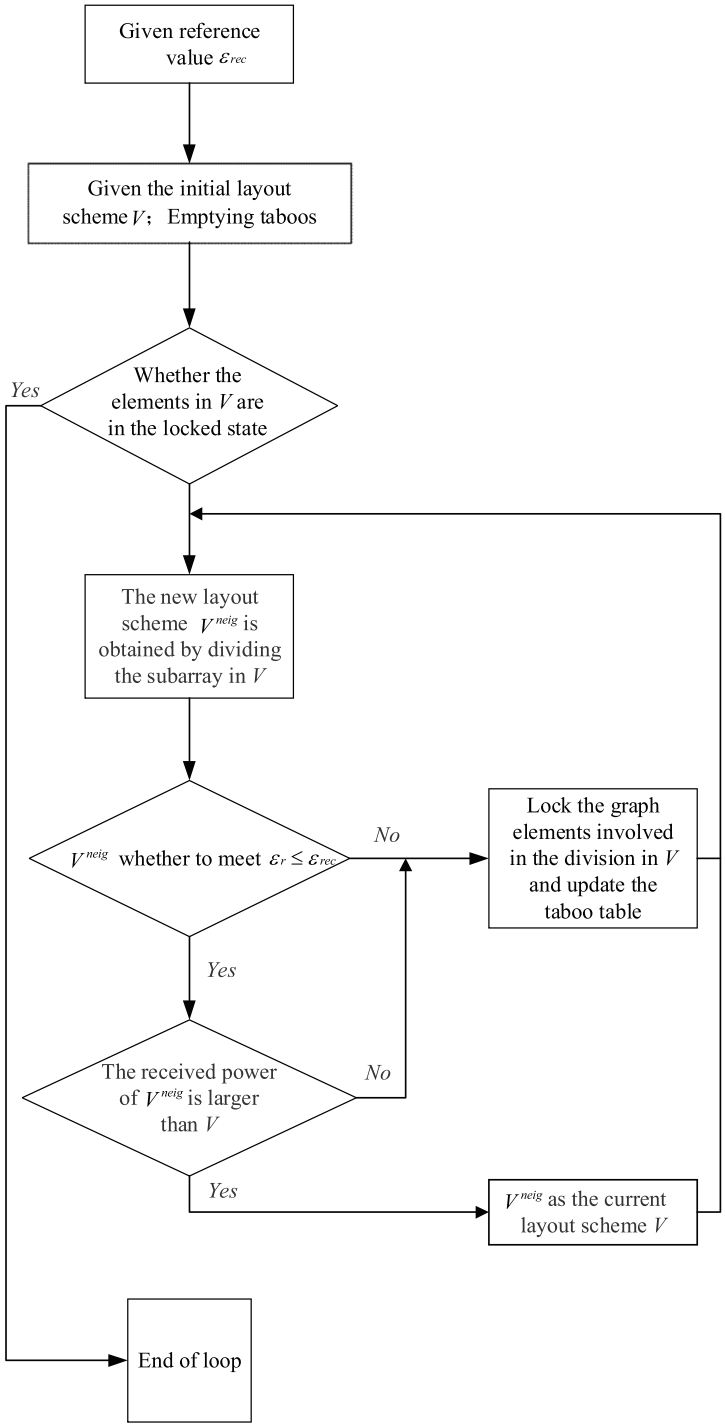

Figure 7. Procedure diagram of the TS algorithm.

In this paper, the frequency is 2.45 GHz. We set the distance H between the transmitter and receiver as 20λ, set the wavelength λ as 1, and set the receiving array aperture diameter as 2.8λ. In addition, because the size of the antenna unit is small relative to the distance between the transmitting and receiving arrays, and the polarization mismatch between the receiving and transmitting arrays has almost no effect on the received power of the subarray, the polarization mismatch factor is set to 1 in the following examples for the relevant calculation.

4.1. Novel Subarray Layout Method

We use the method described in the previous section for subarray layout and set the reference value ε_{rec} as 300 mW, 350 mW, 400 mW, 450 mW, 500 mW, 550 mW. We put the six cases into a relevant simulation analysis study, where different colors indicate different subarray received power values.

In the process of subarray optimization, according to the characteristics of the irradiation power density, the the subarray with smallest size is placed in the center or near the center. As the reference value ε_{rec} increases, the number of large-sized subarrays in the layout decreases, and the large-sized subarray refers to the rectangular subarray without partitioning. However, the number of small-sized subarrays increases. The overall number of subarrays tends to increase, and the cutting density becomes larger. From Fig. 8, we can see that the subarray arrangement has global symmetry, which also greatly

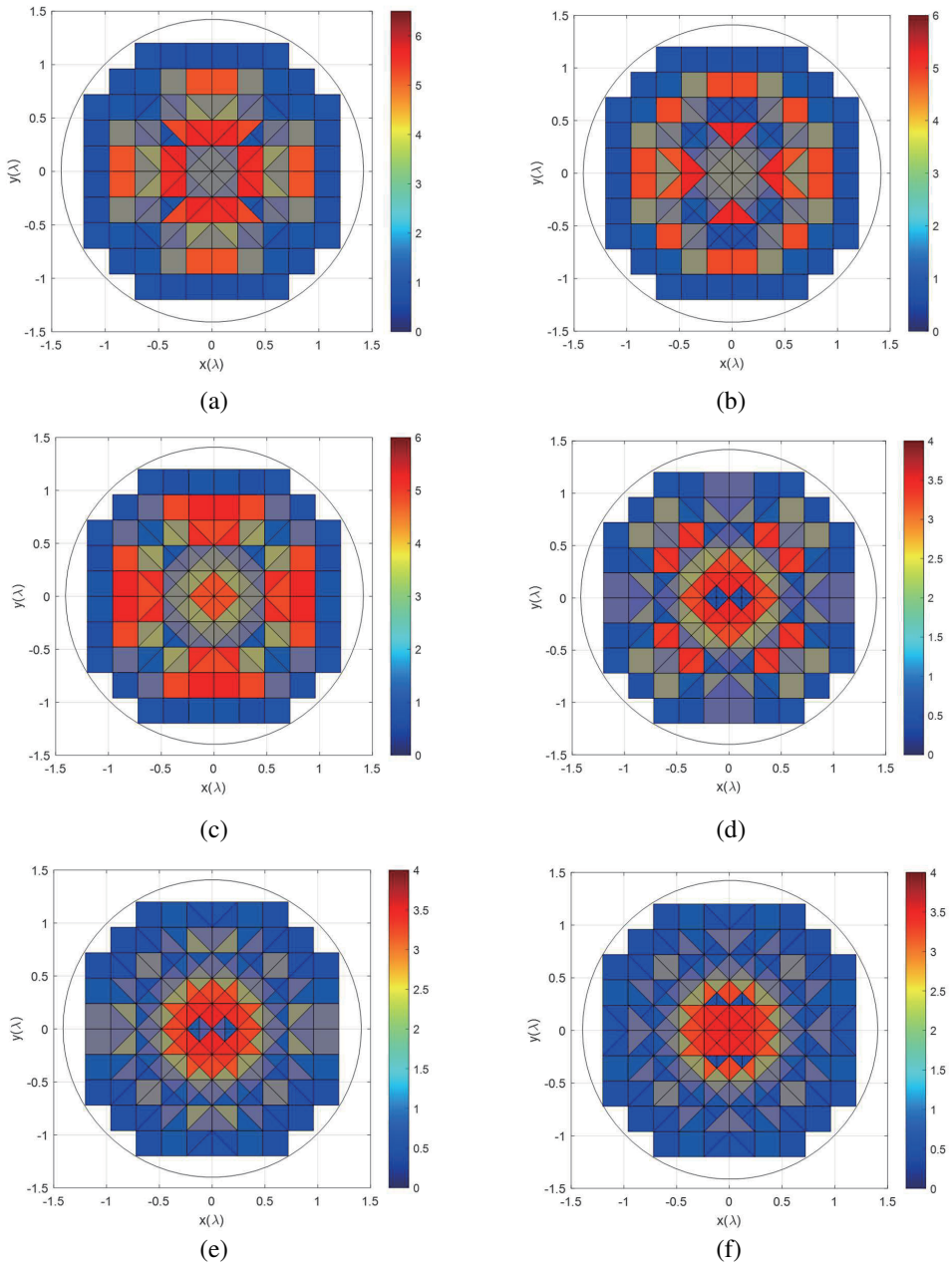

Figure 8. Novel subarray layout for different ε_{rec} cases (a) $\varepsilon_{rec} = 300$ mW, (b) $\varepsilon_{rec} = 350$ mW, (c) $\varepsilon_{rec} = 400$ mW, (d) $\varepsilon_{rec} = 450$ mW, (e) $\varepsilon_{rec} = 500$ mW, (f) $\varepsilon_{rec} = 550$ mW.

reduces the engineering complexity of the subsequent rectifier circuit design. The different subarray types are described in Fig. 2 and Fig. 6 in the previous section. Meanwhile, in order to see more clearly the distribution of received energy in each type of subarray, Fig. 9 shows the actual three-dimensional distribution of received power of the subarray in different ε_{rec} states, and the numerical results are recorded in Table 1. P_r^{rad} in Table 1 indicates the total irradiation power; η represents the total reception efficiency; P_r represents the total actual power received by the receiving array; CV denotes the coefficient of variation of the received power of the subarray, and the scale is 1.

It is easy to see from Table 1 that: (I) ε_{rec} is positively correlated with the number of subarrays, the total irradiated power, and the actual total received power; (II) CV decreases and then increases with ε_{rec}; (III) Total reception efficiency is also positively correlated with ε_{rec}. Only when $\varepsilon_{rec} \geq 450\,\text{mW}$, its growth rate gradually decreases and the data tend to stabilize. Meanwhile, we use the two graphs in Fig. 10 for further analysis.

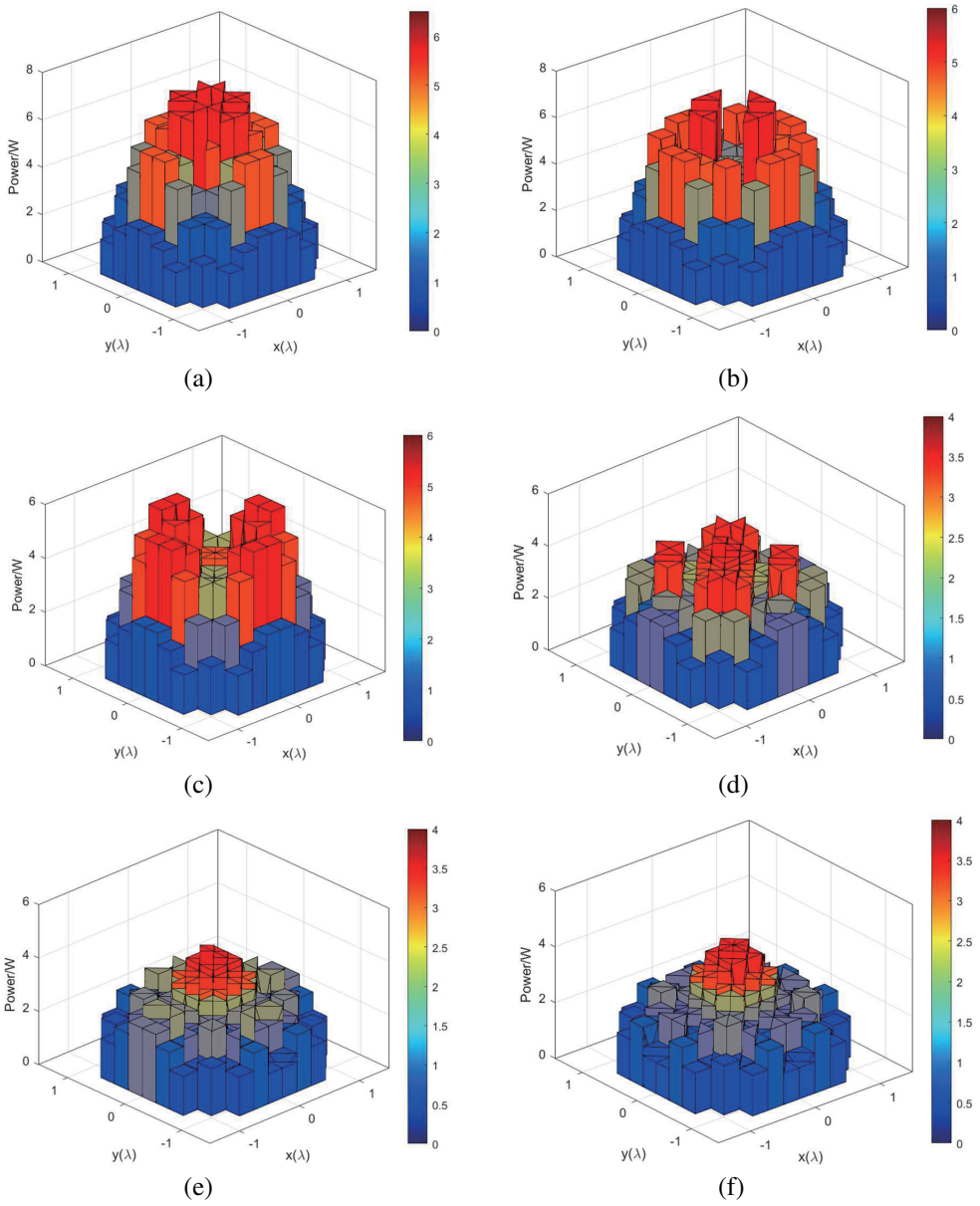

Figure 9. Received power distribution for different ε_{rec} cases (a) $\varepsilon_{rec} = 300\,\text{mW}$, (b) $\varepsilon_{rec} = 350\,\text{mW}$, (c) $\varepsilon_{rec} = 400\,\text{mW}$, (d) $\varepsilon_{rec} = 450\,\text{mW}$, (e) $\varepsilon_{rec} = 500\,\text{mW}$, (f) $\varepsilon_{rec} = 550\,\text{mW}$.

Table 1. Performance analysis of the novel subarray layout scheme for different ε_{rec}.

	M	P_r^{rad} (W)	P_r (W)	η (%)	CV
$\varepsilon_{rec} = 300\,\text{mW}$	136	545.326	417.174	76.5	0.2935
$\varepsilon_{rec} = 350\,\text{mW}$	152	545.710	440.388	80.7	0.2672
$\varepsilon_{rec} = 400\,\text{mW}$	156	546.002	453.182	83.0	0.1926
$\varepsilon_{rec} = 450\,\text{mW}$	192	546.200	460.993	84.4	0.1581
$\varepsilon_{rec} = 500\,\text{mW}$	220	546.307	462.722	84.7	0.2057
$\varepsilon_{rec} = 550\,\text{mW}$	232	546.318	464.371	85.0	0.2502

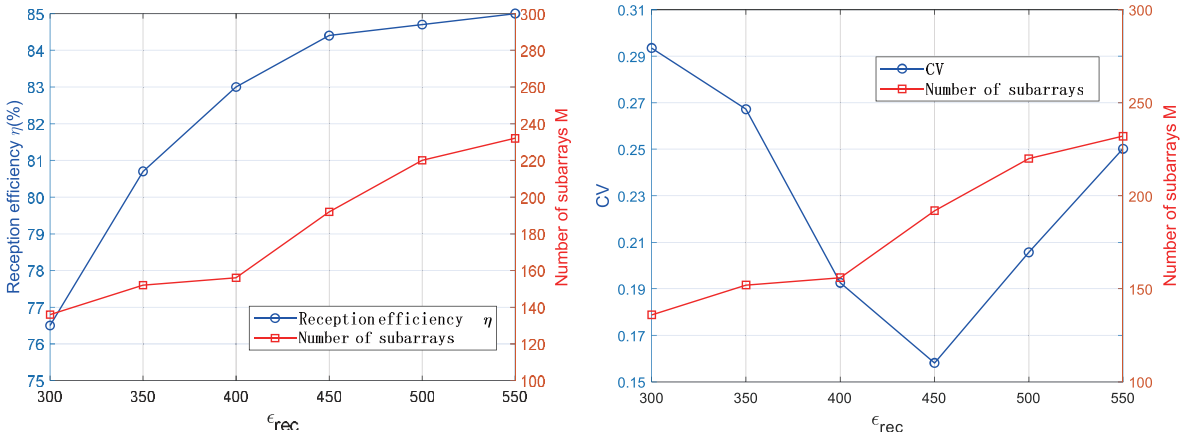

Figure 10. (a) Reception efficiency and total number of subarrays relative to ε_{rec}, (b) Coefficient of variation (CV) and total number of subarrays relative to ε_{rec}.

Combining Fig. 10 and Table 1, we can conclude that the number of subarrays of the receiving array can be effectively controlled by ε_{rec}. When ε_{rec} is in the interval of [300 mW, 450 mW], the number of large-sized subarrays is relatively high, and the value of CV decreases. It also means that the more the number of large subarrays is, the greater the dispersion of the received power of the subarrays is. When ε_{rec} is in the interval [450 mW, 550 mW], due to the inhomogeneity of the irradiated power density, the number of small-sized subarrays increases. And the value of CV increases, indicating that the more the number of small subarrays is, the higher the dispersion of the received power of the subarrays is. CV denotes the ratio of the standard deviation of the received power of the subarray to the average value of the received power. With the increase of ε_{rec}, the number of subarray increases, but the actual total received power increases less and less. Therefore, it will cause the average value of the received power of the subarray to become smaller and smaller. Since the standard deviation must be smaller than the average value, the variation of the standard deviation is also smaller than the variation of the average value. Therefore, the magnitude of the average value will cause a more significant change in the magnitude of the CV. From Table 1 and Fig. 10(a), it is obvious that the growth trend of the actual total received power and total reception efficiency keeps slowing down starting from $\varepsilon_{rec} = 450\,\text{mW}$, thus inferring that CV increases again from 450 mW or more. From Fig. 10(b), we can know that when we control the reference value within a valid range, CV can be extremely small, which also brings some reference for the subsequent design of high conversion efficiency rectifier circuits.

At the same time, the total irradiated power and the actual total received power tend to stabilize with the increase of ε_{rec}, indicating that the control strength of ε_{rec} decreases continuously with the process of its increase. We can also know from Fig. 10(a) that the number of subarrays and the total receiving efficiency η are also positively correlated. With the number of receiving subarrays increasing,

the growth trend of η keeps slowing down. When it is higher than such scale, η does not increase much, and if it is smaller than such scale, the array efficiency decreases sharply.

4.2. Comparison of Rectangular Subarray Partition and Novel Subarray Partition

In order to better highlight the advantages of the novel subarray layout, we then simulate a uniform non-overlapping rectangular subarray partition based on the path traversal algorithm and use the optimization model proposed in this paper, as shown in Fig. 11. The so-called path traversal algorithm, which is similar to the breadth-first search of graph elements, is a generalization of tree traversal by rank [10]. In addition, we record the numerical simulation results in Table 2.

Different colors in Fig. 11 represent different subarray received power values. The trend of each

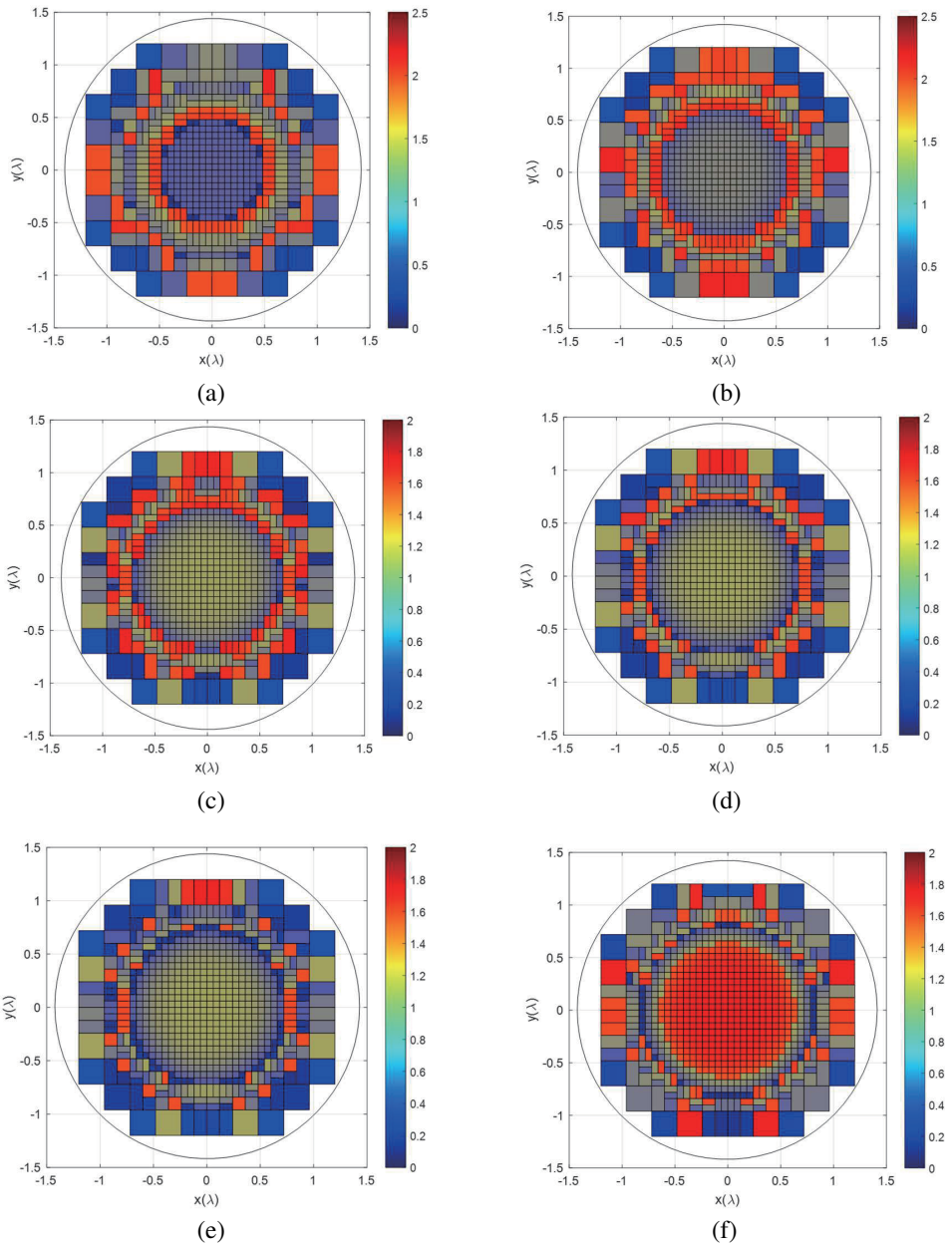

Figure 11. Subarray layout results for different ε_{rec} cases (a) $\varepsilon_{rec} = 300\,\text{mW}$, (b) $\varepsilon_{rec} = 350\,\text{mW}$, (c) $\varepsilon_{rec} = 400\,\text{mW}$, (d) $\varepsilon_{rec} = 450\,\text{mW}$, (e) $\varepsilon_{rec} = 500\,\text{mW}$, (f) $\varepsilon_{rec} = 550\,\text{mW}$.

Table 2. Performance analysis of the subarray layout scheme for different ε_{rec}.

	M	P_r^{rad} (W)	P_r (W)	η (%)	CV
$\varepsilon_{rec} = 300\,\text{mW}$	510	655.208	507.131	77.4	0.3539
$\varepsilon_{rec} = 350\,\text{mW}$	584	657.813	536.118	81.5	0.3058
$\varepsilon_{rec} = 400\,\text{mW}$	644	658.371	552.373	83.9	0.2816
$\varepsilon_{rec} = 450\,\text{mW}$	684	659.457	554.603	84.1	0.1953
$\varepsilon_{rec} = 500\,\text{mW}$	714	659.899	558.275	84.6	0.2864
$\varepsilon_{rec} = 550\,\text{mW}$	740	661.232	560.725	84.8	0.3287

part of the parameters is similar to the novel subarray layout scheme. But the obvious difference is that the number of subarrays used in this type of layout is a lot. The division between quadrant and quadrant is not symmetrical. Additionally, the energy distribution is not uniform, and CV obtained is also much higher than the novel subarray layout. It indicates that the subarray received power dispersion is greater. In order to further show CV variation of the two types of subarray layout, we plot the curve shown in Fig. 12. $CV1$ represents the coefficient of variation of the novel subarray layout, and $CV2$ represents the coefficient of variation of the subarray layout in Fig. 11.

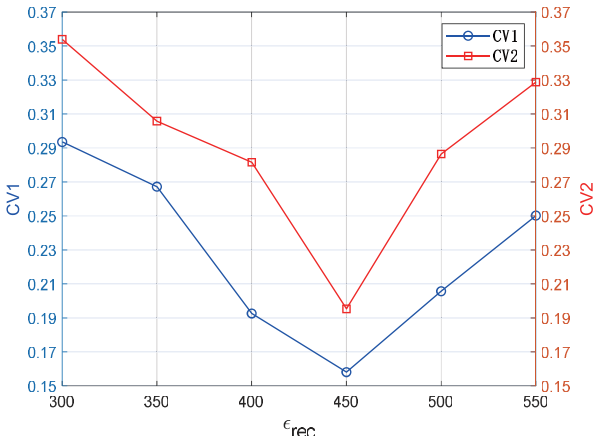

Figure 12. Comparison of two types of CV results.

Both reach the extreme minimum when $\varepsilon_{rec} = 450\,\text{mW}$. At this moment, $CV1 = 0.1581$ and $CV2 = 0.1953$. In all the other reference value cases, $CV1$ is also smaller than $CV2$, and the values of the reception efficiency of the two layout methods in the six cases are [76.5, 80.7, 83.0, 84.4, 84.7, 85.0], [77.4, 81.5, 83.9, 84.1, 84.6, 84.8]. The reception efficiency of the novel subarray layout is lower than that of the second subarray layout when $\varepsilon_{rec} \leq 400\,\text{mW}$, but it does not decrease too much. The efficiency is slightly higher when $\varepsilon_{rec} \geq 400\,\text{mW}$. This also proves that the novel subarray layout scheme can make the subarray received power less discrete and better homogenized when ensuring relatively higher reception efficiency, while the smaller number of subarrays also reduces the complexity of the rectifier circuit.

4.3. Comprehensive Comparison of the Current Receiving Rectifier Array Layout

We select representative data from the above two array layouts, rectangular subarray partition and novel subarray partition selected when $\varepsilon_{rec} = 450\,\text{mW}$, and then compare the RF synthesis layout and DC synthesis layout. RF synthesis and DC synthesis can be combined with references [9, 10], and the data are recorded in Table 3, where P_r_mean and P_r_std denote the average value of subarray received power and the standard deviation of subarray received power, respectively.

Table 3. Comparison of array layout.

	Ref. [10]		Subarray Layout	
	RF Synthesis	DC Synthesis	Rectangular Subarray Partition	Novel Subarray Partition
element or subarray number	1	1440	684	192
P_r^{rad} (W)	578	578	659.457	546.200
P_r (W)	246	527	554.603	460.993
η (%)	42	90	84.1	84.4
P_r_mean (W)	---	365	0.8108	2.4010
P_r_std (W)	---	256	0.1584	0.3796
CV	---	0.70	0.1953	0.1581

In Table 3 we compare RF layout and subarray layout. Although the units used in the former are very few, the efficiency is very low. Then we compare DC layout and subarray layout. Although the former can get a higher reception efficiency, the coefficient of variation reaches 0.70; the received power dispersion is very high; and the number of units is a lot, which is very unfavorable to the design of high conversion efficiency rectifier circuit. So it highlights that the subarray layout is more suitable as the layout of the receiving antenna array. It is also shown through the data that the novel subarray layout based on the TS algorithm has the significant advantage of low cost and low dispersion compared with the rectangular subarray layout based on the traditional path traversal algorithm.

Subarray partition has innovative implications, but there are also some areas that require additional consideration. For example, the number of partitions will increase, which will cause a certain loss of power, thus affecting the overall reception efficiency. It is relatively difficult to make the reception efficiency more than 90 percent. However, this method solves the problem of nonuniform irradiation power density. Receiving arrays including a single RF-to-DC converter have the disadvantage of requiring a full RF feed network (working at high power levels, possibly) able to track the transmitter beam. Moreover, they are less robust to diode failures, since the power conversion is carried out in a single collecting point. To reduce such drawbacks, subarray-based architectures have been proposed. In these architectures, the overall receiving layout is divided into subarrangements whose gathered signals are (locally) combined in RF and then converted to DC. Subarray partition can solve exactly these problems. To sum up, the benefits of using subarray layout are a bit more.

5. CONCLUSION

In this paper, a novel subarray layout model is proposed for the problem of high dispersion of received power in rectified antenna arrays. Firstly, the subarray received power calculation model is used as the basis, and the optimization model is established with the goal of homogenization of the received power of the subarray. Subsequently, the global solution is performed with the TS algorithm, and the optimal layout of the subarray is obtained by simulation. Secondly, through numerical experiments first compare the uniform non-overlapping triangular subarray partition method to the uniform non-overlapping rectangular subarray partition method, highlighting the superiority of the novel subarray layout with low power dispersion and low complexity. Finally, the comprehensive comparison with the current receiving rectifier antenna array layout shows that the uniform non-overlapping triangular subarray partition is more suitable as the layout of the Microwave Power Transmission Receiver. It also verifies the feasibility of the subarray partition model designed in this paper again.

ACKNOWLEDGMENT

This work was supported by the National Natural Science Foundation of China (Grant No. 51877151).

REFERENCES

1. Massa, A. and F. Viani, "Array designs for long-distance wireless power transmission: State-of-the-art and innovative solutions," *Proceedings of the IEEE*, Vol. 101, No. 6, 1464–1481, 2013.
2. Brown, W. C., "The history of power transmission by radio waves," *IEEE Transactions on Microwave Theory Techniques*, Vol. 32, No. 9, 1230–1242, 1984.
3. Shidujaman, M., H. Samani, and M. Arif, "Wireless power transmission trends," *International Conference on Informatics*, Dhaka, Bangladesh, 2014.
4. Sasaki, S., K. Tanaka, and K. Maki, "Microwave power transmission technologies for solar power satellites," *Proceedings of the IEEE*, Vol. 101, No. 6, 1438–1447, 2013.
5. Liu, X., X. Zhang, and H. Yan, "Research of subarray partition in optically phased array radar," *Applied Science & Technology*, 2006.
6. Wan, S. and K. Huang, "Methods for improving the transmission-conversion efficiency from transmitting antenna to rectenna array in microwave power transmission," *IEEE Antennas and Wireless Propagation Letters*, Vol. 17, No. 4, 538–542, 2018.
7. Song, C. M., S. Trinh-Van, S. H. Yi, et al., "Analysis of received power in RF wireless power transfer system with array antennas," *IEEE Access*, Vol. 9, 76315–76324, 2021.
8. Xiong, Z., Z. Xu, S. Chen, et al.,"Subarray partition in array antenna based on the algorithm X," *IEEE Antennas and Wireless Propagation Letters*, Vol. 12, No. 12, 906–909, 2013.
9. Ugur, O., C.-C. Chen, and J. L. Volakis, "Investigation of rectenna array configurations for enhanced RF power harvesting," *IEEE Antennas and Wireless Propagation Letters*, Vol. 10, No. 10, 262–265, 2011.
10. Yao, Y., L. W. Song, and Y. L. Liu, "Subarray partition design of receiving antenna for microwave power transmission," *2019 IEEE International Conference on Microwave and Millimeter Wave Technology (ICMMT)*, 1–3, Guangzhou, China, February 2020.
11. Li, J., J. Pan, and X. Li, "A novel synthesis method of sparse nonuniform-amplitude concentric ring arrays for microwave power transmission," *Progress In Electromagnetics Research C*, Vol. 107, 1–15, 2021.
12. Yang, Y., J. Li, L. Li, and B. Zhang, "5.8 GHz circularly polarized rectenna with harmonic suppression and rectenna array for wireless power transfer," *IEEE Antennas and Wireless Propagation Letters*, Vol. 17, No. 7, 2018.
13. Li, J. and Y. Tan, "A novel receiving antenna array layout method for microwave power transmission," *Progress In Electromagnetics Research M*, Vol. 108, 187–200, 2022.
14. Stark, L., "Microwave theory of phased array antenna — A review," *Proceedings of the IEEE*, Vol. 62, 1661–1701, 1974.
15. Qiang, C., C. Xing, and F. Pan, "A comparative study of space transmission efficiency for the microwave wireless power transmission," *IEEE Asia-Pacific Microwave Conference*, 1–3, Nanjing, China, 2015.
16. Li, X., K. M. Luk, and B. Duan, "Multiobjective optimal antenna synthesis for microwave wireless power transmission," *IEEE Transactions on Antennas and Propagation*, Vol. 67, No. 4, 2739–2744, 2019.
17. Takahashi, T., T. Mizuno, M. Sawa, et al., "Development of phased array for high accurate microwave power transmission," *IEEE MTT-S International Microwave Workshop Series on Innovative Wireless Power Transmission: Technologies, Systems, and Applications*, 157–160, Kyoto, Japan, 2011.
18. Zbitou, J., M. Latrach, and S. Toutain, "Hybrid rectenna and monolithic integrated zero-bias microwave rectifier," *IEEE Transactions on Microwave Theory Techniques*, Vol. 54, No. 1, 147–152, 2006.
19. Bui-Van, H., M. Arts, C. Craeye, et al., "On the maximum absorbed power in receiving antenna arrays," *IEEE Transactions on Antennas and Propagation*, Vol. 67, No. 3, 1993–1995, 2019.

20. Zinka, S. R. and J. P. Kim, "On the generalization of taylor and bayliss N-bar array distributions," *IEEE Transactions on Antennas and Propagation*, Vol. 60, No. 2, 1152–1157, 2011.
21. Greene, C. E., *Area of Operation for a Radio-Frequency Identification (RFID) Tag in the Far-Field*, 2006.
22. Colin, R. E., *Antenna and Radiowave Propagation*, McGraw-Hill, Inc., 1985.